applied sciences

MDPI

Article

Design of a Planar Cable-Driven Parallel Robot for Non-Contact Tasks

Valentina Mattioni †, Edoardo Ida' *,† and Marco Carricato

Department of Industrial Engineering, University of Bologna, Viale Risorgimento 2, 40136 Bologna, Italy; valentina.mattioni@unibo.it (V.M.); marco.carricato@unibo.it (M.C.)

* Correspondence: edoardo.ida2@unibo.it

† These authors contributed equally to this work.

Abstract: Cable-driven parallel robots offer significant advantages in terms of workspace dimensions and payload capability. Their mechanical structure and transmission system consist of light and extendable cables that can withstand high tensile loads. Cables are wound and unwound by a set of motorized winches, so that the robot workspace dimensions mainly depend on the amount of cable that each drum can store. For this reason, these manipulators are attractive for many industrial tasks to be performed on a large scale, such as handling, pick-and-place, and manufacturing, without a substantial increase in costs and mechanical complexity with respect to a small-scale application. This paper presents the design of a planar overconstrained cable-driven parallel robot for quasi-static non-contact operations on planar vertical surfaces, such as laser engraving, inspection and thermal treatment. The overall mechanical structure of the robot is shown, by focusing on the actuation and guidance systems. A novel concept of the cable guidance system is outlined, which allows for a simple kinematic model to control the manipulator. As an application example, a laser diode is mounted onto the end-effector of a prototype to perform laser engraving on a paper sheet. Observations on the experiments are reported and discussed.

Keywords: cable-driven parallel robots; overconstrained robots; design; non-contact operations

Citation: Mattioni, V.; Ida', E.; Carricato, M. Design of a Planar Cable-Driven Parallel Robot for Non-Contact Tasks. *Appl. Sci.* **2021**, *11*, 9491. https://doi.org/10.3390/app11209491

Academic Editor: Alessandro Gasparetto

Received: 19 September 2021
Accepted: 23 September 2021
Published: 13 October 2021

1. Introduction

Cable-driven parallel robots (*CDPRs* in short) combine the successful features of parallel manipulators with the benefits of cable transmissions. The payload is divided among light extendable cables, resulting in an energy-efficient system that can achieve high acceleration of the end-effector (*EE*) over a remarkably large workspace. From a structural point of view, a *CDPR* is formed by a set of actuation units, usually fixed to a frame, and a mobile platform, working as *EE* [1]. The cables, driven by the actuation units, are guided inside the robot workspace (*WS*) using a guidance system, and then connected to the mobile platform. The variation of cable lengths is responsible for the *EE* displacement throughout the robot *WS*. These features result in easily reconfigurable systems, where the *WS* can be modified by relocating the actuation and/or guidance units [2].

Nevertheless, the use of *CDPRs* in industrial environments is still limited, mainly due to the drawbacks of employing flexible cables. Indeed, cables impose unilateral constraints that can only exert tensile forces and, consequently, the *EE* cannot withstand any arbitrary external action. In addition, the viscoelastic nature of cables can cause their elongation under prolonged load application [3]. This highly non-linear behavior complicates the control of the robot and the estimation of the actual cable lengths, and therefore the determination of the platform pose through direct kinematics. To enhance the robot controllability, *CDPRs* can be overconstrained by employing a number of cables higher than the degrees of freedom (*DoFs*) of the *EE*. This allows cables to pull one against the other and to keep the overall system controllable over a wide range of externally applied loads. In other cases, to increase accessibility and reduce hardware complexity,

suspended architectures with less cables than *EE DoFs* can be used, though they are more difficult to control [4,5].

Thanks to their simple architecture, high reconfigurability, easy deployability, and large workspace, *CDPRs* have been proposed in many fields of application: entertainment [6,7], logistics [8], construction [9–11], maintenance [12,13], to name a few. In general, it is possible to design a general-purpose machine that can be dedicated to different tasks by changing the *EE* tool [14,15] or, in alternative, a *CDPR* for a specific purpose can be developed. In the second case, the robot geometry, the number and configuration of cables, and, consequently, additional design constraints are established by the final task. This is the case of the deployable *CDPR* in [16]: the suspended architecture and the *EE* self-deployability ensure the high orientational capability required for the laser scanning of low-accessibility environments. As an additional example, the storage-retrieval *CDPR* in [8] is equipped with eight cables, despite the planar nature of the robot task, in order to provide a suitable machine stiffness and prevent platform tilt.

Usually, if the task requires a specific motion pattern of the *EE*, it is possible to act in two different ways to limit the *EE* range of motion. First, an external means, which physically constrains the *EE*, can be employed. This happens with the *CDPR* Pickable [17], whose *EE* is constrained to slide on a planar surface thanks to an air-bearing system. Likewise, in [13], the *EE* of the robot moves in direct contact with the building façade to perform window cleaning operations. The contact of the *EE* with the environment requires specific contact models [18], and suitable force-control strategies [19]. For the Pickable robot, undesired phenomena, such as friction, are significantly reduced by using air bearings, whereas, for the cleaning robot, friction is part of the process itself. A different approach for constraining the *EE* motion consists in adopting special cable configurations, such as the parallelogram arrangements inspired by delta robots [20–22]. This expedient allows obtaining a translational motion of the *EE* without any external constraint, provided that all cables are taut. This is useful in the case of large-scale industrial tasks, such as pick-and-place and warehousing [23], or operations that need deployable systems, such as rescue and contour crafting [24,25].

The parallelogram arrangement strategy can also be applied in non-contact tasks where the *EE* must move on a prescribed vertical plane without interacting with the surrounding environment. This is the case of welding, laser engraving, thermal treatment, and decoration or inspection of building façades, to name a few. This paper focuses on the design of a *CDPR* for this kind of applications. Specifically, an overconstrained planar machine is presented. This prototype employs a parallelogram cable arrangement to constrain the *EE* to move on a vertical plane. Four cables, closed in a parallelogram loop, are used to control the mobile platform's three degrees of freedom (*DoFs*). The cable guidance system comprises a pair of swivel pulleys whose swivel axes are orthogonal to the work surface: the intersections of these swivel axes with the work surface effectively define the cable proximal and distal points. Each cable loop is driven by one winch, whose drum has two helicoidal starts. Each winch includes a rotary encoder for cable length control. In addition, the pulley swivel axes are equipped with rotary encoders to achieve redundant kinematic measures, and cable tensions are measured with shear beam load cells integrated into the proximal anchor systems. Like other planar *CDPR* that share the idea of parallelogram mechanisms [23,26], this system allows the platform to move on a defined plane, excluding low-amplitude oscillatory motions induced by external disturbances [27,28]. On the other hand, unlike the others, the proposed system shows three advantages: the use of a single cable loop, instead of two separate cables, ensures that the parallel cable segments are in tension when controlled by a single actuator, thus reducing the number of actuators to be used; the cable anchor system includes a measurement unit to continuously monitor cable tensions and cable angles with respect to the frame; the mounting arrangement of the swivel pulleys allows to estimate the cable lengths as distances between two precisely defined points, which are the intersections between the swivel axes and the work plane, without introducing geometrical approximations.

Consequently, a simple geometric model can be adopted to control the *CDPR* without inherent geometrical errors.

The paper is organized as follows. The main aspects to be taken into consideration for the mechanical design of a *CDPR* are described in Section 2. Then, the design of the planar overconstrained *CDPR* prototype is presented in Section 3, focusing on the actuation and guidance system, and the influence of the kinematic model. In Section 4, as an application example, an experiment of the robot performing laser engraving is reported and discussed. Lastly, some conclusions are drawn.

2. Design Strategies

In most cases, cables are driven by actuators that are placed on a fixed base. Sometimes, if deployability is a requirement, they can be attached to mobile vehicles [24] or placed on the mobile platform [29]. A guidance system is used to convey cables from the actuators to the mobile platform. Many authors analyzed the design process of *CDPRs* and identified several methods for optimizing their structure and dimensions [1,30]. For a given criterion (i.e., workspace dimension, accuracy, stiffness, orientation capability), optimization procedures help determine the geometry of the *CDPR*, including the number of cables, position of cable anchor points, and platform and frame shapes [2,15,31]. Once the architecture is known, the hardware design requires developing three distinct systems: the actuation unit, the guidance system, and the mobile platform. These systems can be equipped with suitable sensors, to monitor the robot performance and obtain feedback on relevant control variables. The two most notable examples are cable lengths, which are usually estimated by using angular sensors mounted on the actuation unit motors, and cable tensions, whose measurement involves integrating force sensors in the actuation unit, guidance system, or *EE* [1].

This section shows how specific design techniques can help keep the robot model and control as simple as possible without introducing geometrical approximations. Usually, a simplified kinematic model, called standard in the following, is adopted. This model considers cables inextensible and massless and, thus, treated as line segments between two points, one on the mobile platform and the other on the frame (distal and proximal anchor points, respectively). The former is usually assumed to be fixed with respect to the moving platform, whereas the latter is fixed with respect to the robot frame. These assumptions neglect not only all effects caused by the elastic nature of cables, which may be negligible in some small-to-medium-scale applications, but also the kinematics of the guidance system. Geometrical-model errors can be limited by accounting for the pulley geometry [4,32], but the model and control complexity is usually increased. As an alternative, if the standard kinematic model is to be used without inherent geometrical errors, special design techniques of the actuation units and guidance systems can be used, as discussed in the following.

2.1. Actuation Unit

The most appropriate type of actuation is chosen depending on the *EE* motion pattern and *WS* size, defined by the task [1,33]. A rotary actuation system generally consists of a servo-actuated winch where the cable is coiled onto a cylindrical drum. This solution is easy to implement but can result in low robot position accuracy since it introduces several errors when estimating cable lengths [34]. Lengths are computed by measuring the rotation of the motor and, thus, they depend on the drum design and cable arrangement on it. Linear actuation systems reduce cable-length estimation errors, but they usually limit the size of the achievable *WS* [35], or increase cable wear [34].

A solution could be to adopt a rotary actuation system designed to be as close as possible to the model intended for its control. The main drawback of the rotary actuation, if a simple lifting winch is considered, is the fact that the cable exit direction from the drum varies, even unpredictably, as the motor rotates: this results in a non-linear transmission ratio between the motor angle and the cable length, which is usually undesirable. A constant transmission ratio can be obtained (i) by avoiding the cable overlapping onto the

drum surface, (ii) by suitably grooving the drum to accommodate the cable, which is also desirable for reducing cable wear [36], and (iii) by constraining the cable to exit the drum in a fixed, known, direction. There are several solutions in the literature to achieve such desired design requirements (Figure 1).

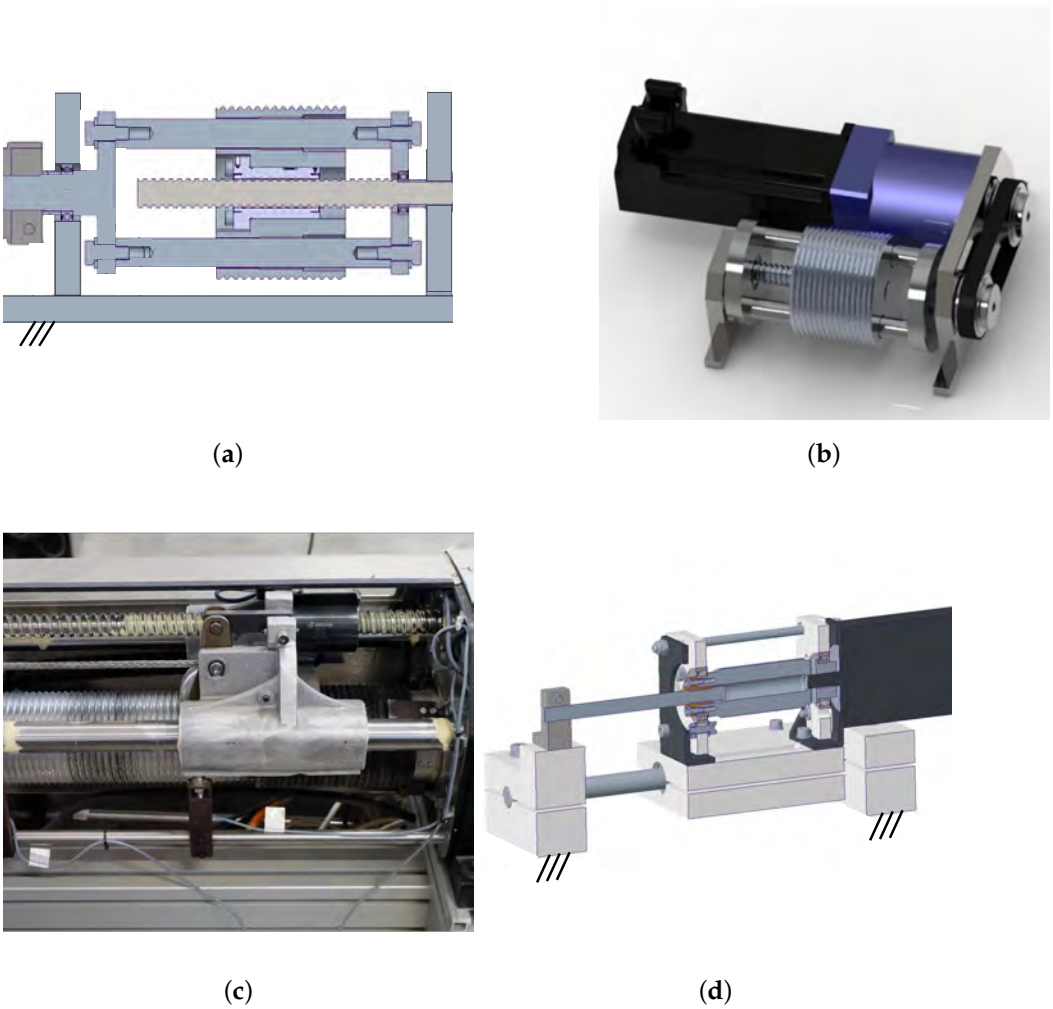

(**a**) (**b**)

(**c**) (**d**)

Figure 1. Winch models. (**a**) Cross section of a rototranslating drum. (**b**) Rendering of a winch with rototranslating drum kinematically equivalent to the ones in [37,38]. (**c**) Close-up view of a winch of the Ipanema *CDPR* family [14]. (**d**) Winch with translational motor-drum.

It is possible to rototranslate the drum [16,37,38] so that the cable exit point from the drum, and consequently its direction, is kept fixed with respect to the winch frame, while the cable is coiled and uncoiled. This is usually achieved by employing screw/nut joints to convert the rotational motion of the motor into rotational and translational motion of the drum, and allowing the drum to translate by mounting it on a passive prismatic joint. In [38] the drum houses a nut and two pairs of cylindrical bearings. Two rods, which are coupled with the motor shaft, parallel to the drum axis, but mounted with a radial offset with respect to the drum, pass through the bearings, thus transmitting the rotational motion, but allowing the drum to translate. The translation is caused by the drum nut being joined with a screw, which is fixed on the winch frame: a cross section of the drum system is shown in Figure 1a. The main advantages of this solution are compactness and mechanical simplicity, but this design suffers from one main drawback, namely the rods used for transmitting the motor rotations pass through the drum, thus the latter diameter needs to be large. An example of this design is shown in Figure 1b, where a timing belt is used to transmit motion from the motor to the drum, as in [37].

As an alternative, in [14] an auxiliary cable guiding device equipped with a pulley (*spooling helper*) continuously follows the variable cable exit point on the rotating drum (Figure 1c) by translating parallel to the drum axis, to ensure that the direction of the cable connecting the drum and the spooling helper is constant. The spooling helper is mounted on a support equipped with a nut and a pair of bearings, and thus slides with respect to fixed rods, driven by a screw, which is ultimately connected to the drum with a synchronous belt. Given its footprint, this solution has the primary benefit of allowing very long cables to be stored onto the drum. Still, an additional mechanical transmission, such as a timing belt, is always required to transmit drum motion to the screw.

A different solution allows the translation of the entire motor-drum system on a linear guide [39], similar to the design shown in Figure 1d. This solution has the advantage of being particularly simple and cheap, since the drum is directly connected to the motor, and the drum supports are connected to a carriage. Still, the motor mass, which needs to be translated, may limit the system's dynamic performance.

2.2. Guidance System

One of the main advantages of *CDPRs* is the possibility to locate the actuation units almost anywhere. This is possible thanks to the cable guidance system that conveys the cable, from the actuator, through the prescribed anchor points on the frame (proximal) to the anchor point on the platform (distal). For the standard model to be respected, without introducing geometrical-model errors, the cable anchor points need to be geometrically determined. An extensive review of possible construction solutions is reported in [1], where a distinction is made between the proximal and distal anchor systems.

The mechanical devices that compose the proximal guidance system should allow for large deflection angles and at the same time determine the anchor point position. Swivel (or panning) pulleys and eyelets are primarily used for this purpose. Eyelets allow for the approximate definition of a point and significant cable orientation, but cause high cable wear [40]. However, they are employed in many *CDPRs* thanks to their simplicity, and the possibly low geometrical error introduced, if the *CDPR* workspace is large [16,38,41]. Figure 2 shows the use of eyelets as proximal anchor points on the fixed frame of the *CDPR* prototype presented in [16]. Conversely, swivel pulleys can reduce cable wear and still allow for orientation in a broad direction range, since, unlike classical fixed pulleys (Figure 3a), they can rotate about an axis tangent to the pulley groove, the swivel axis (Figure 3b). This kind of solution is adopted in [39,42], and an example of exit point layout is shown in Figure 4. In general, the presence of pulleys in the guidance system makes the system reliable, but complicates the geometrical model of the robot. This issue can be faced in two ways: by adopting a more complex model, which includes pulley kinematics for *CDPR* control [4,32,43], or by ignoring the actual geometry of the system, and accepting several modeling errors. Otherwise, particular layout and orientations of the pulley system must be adopted.

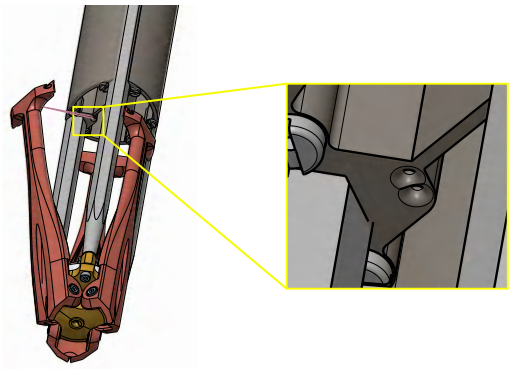

Figure 2. Model of the eyelet exit point of the *CDPR* laser scanner in [16].

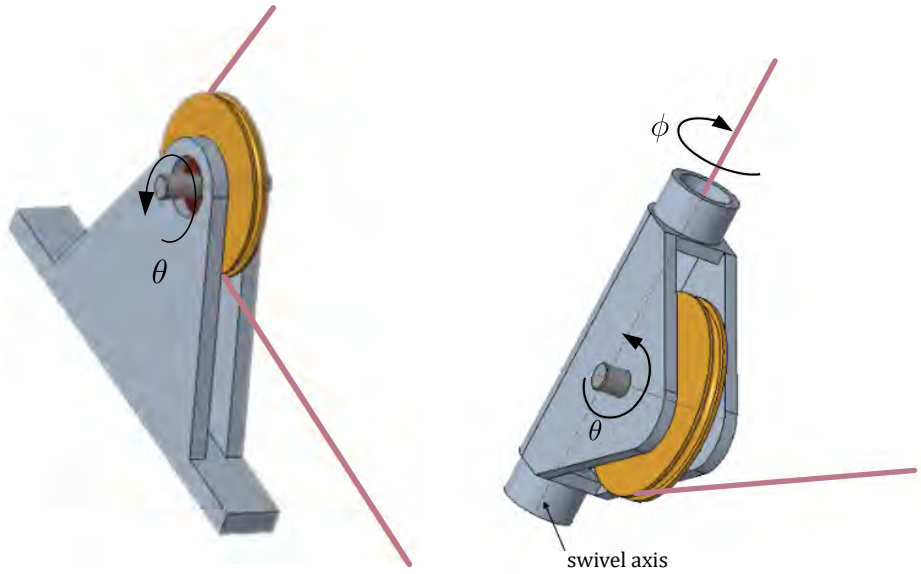

Figure 3. 3D model of pulley transmissions. (**a**) Fixed pulley. (**b**) Swivel pulley.

Figure 4. Application of swivel pulleys for cable proximal anchor point.

On the platform, at the distal anchor points, cables can be knotted to a fixture (i.e., an eyelet or a hook) or anchored to a universal joint: both these options allow to define a fixed point with respect to the platform. The knot solution is preferred for its simplicity (Figure 5) [16,44], but it is neither accurate nor reliable for long-term use. On the other hand, the universal joint (Figure 6) is more precise but complex and more expensive. Pulleys can also be employed if the cable needs to be deflected and not fixed at the distal anchor point. In [45], a pulley system is used at the distal anchor point on the platform to compensate for the effect of the proximal swiveling pulley geometrical model.

(**a**) (**b**)

Figure 5. Cable knotted at the anchor point on the platform of the *CDPR* laser scanner [16]. (**a**) Platform overview. (**b**) Knot detail.

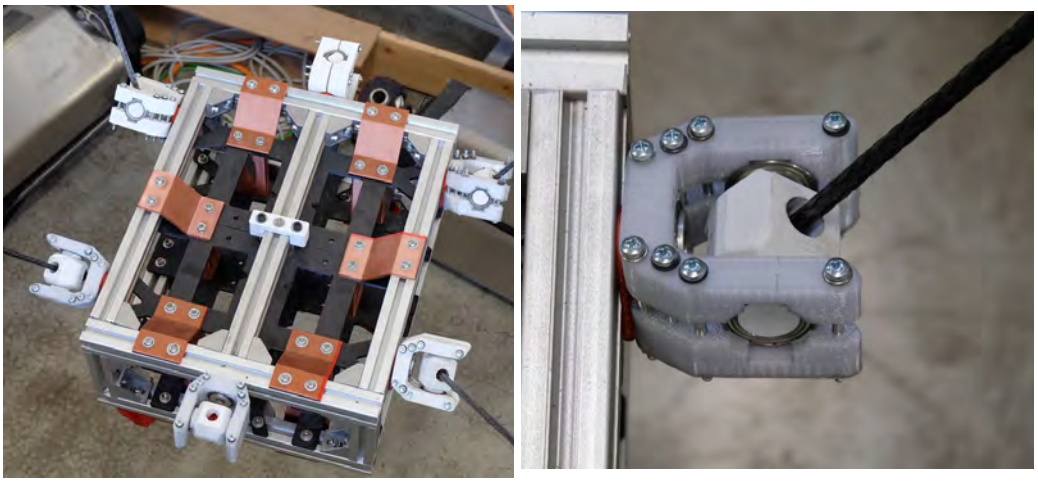

(**a**) (**b**)

Figure 6. Prototypal universal joint at the anchor point on the platform of a *CDPR*. (**a**) Platform overview. (**b**) Universal joint detail.

3. Mechanical Design

The prototype presented in this section is devoted to non-contact tasks, such as laser engraving, welding, thermal treatment, decoration, and inspection of vertical surfaces, such as building façades. Thus, the main design requirements are the following: (i) it should present a planar vertical workspace, which should be easily scaled upon the redefinition of the installation locations of the guidance systems, (ii) the tool mounted on the platform should be interchangeable.

The 3D model of the designed prototype is shown in Figure 7. The machine frame (1) is formed by aluminum profiles that define the robot installation (and *WS*) limits. An actuation (2) and a proximal guidance unit (3) are placed at each of the four corners of the frame to coil and uncoil four cables and convey them to the distal guidance unit (4) attached to the mobile platform (5). The platform has $n = 3$ *DoFs* in the plane, thus, a 4-cable architecture results in an overconstrained manipulator. The constraint redundancy allows firstly to obtain a wider *WS* and then improve the *EE* controllability. Redundant

actuated cables make them pull one against the other to keep the overall system under tension. Reconfigurable anchor points also characterize the prototype: cables can be arranged in a standard (Figure 8a) or crossed (Figure 8b) layout by simply un-mounting and re-mounting the distal guidance unit. As shown in Figure 8, each swivel pulley (1) on the platform, which forms the distal anchor point, can be translated into slots (2) on the support (3); the equivalent operation can be done on the proximal anchor systems on the frame. The crossed layout aims to improve the platform's orientation capability [46], if required by the task, and to withstand external torques induced by gravity (if the tool is not mounted in a barycentric position) or external disturbances.

The actuation units and guidance systems are the same for each cable, and they are described in the following subsections.

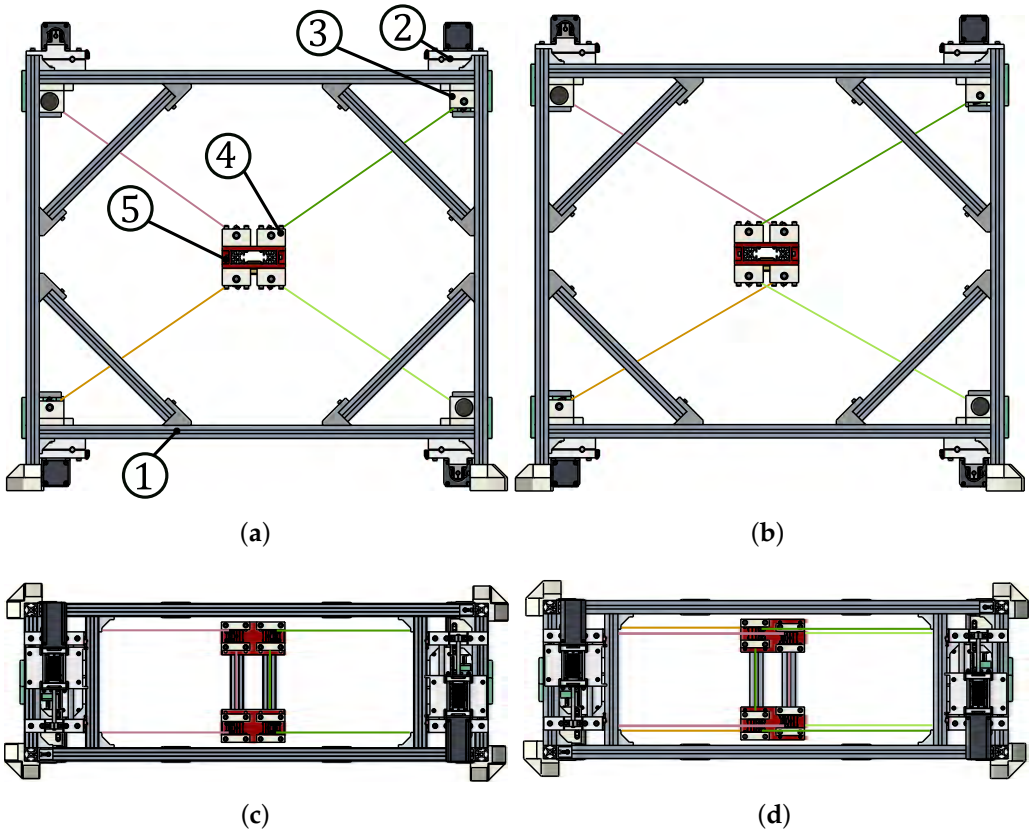

Figure 7. Planar 4-cable *CDPR* prototype with two cable arrangements: (1) frame, (2) actuation unit, (3) proximal guidance unit, (4) distal guidance unit, (5) platform. (**a**) Standard layout, front view. (**b**) Crossed layout, front view. (**c**) Standard layout, top view (**d**) Crossed layout, top view.

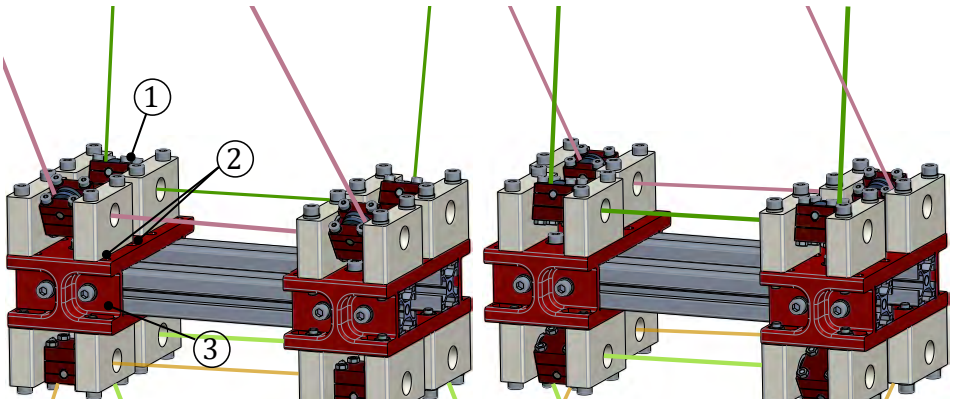

Figure 8. Reconfigurable distal anchor points on the mobile platform: (1) swivel pulley, (2) slots for the translation of the swivel pulley, (3) platform support. (**a**) Standard layout. (**b**) Crossed layout.

3.1. Actuation Unit

The cable actuation unit is a servo-actuated winch where both the motor and the drum translate along a linear guide during the motor rotation (Figure 9). As described in Section 2.1, this design choice limits the overall machine cost, at the price of poorer actuator dynamic performances: given the quasi-static requirement for the robot operation, this design choice was deemed the best. In addition, to further limit the robot cost, most components were produced by Fused Deposition Modeling (FDM) technology using PETG as base material. The choice of a rotary actuation, instead of a linear one, is supported by the project requirements reported in Section 3. In particular a rotary actuator allows for easy scalability in case of wide-workspace applications and field deployability.

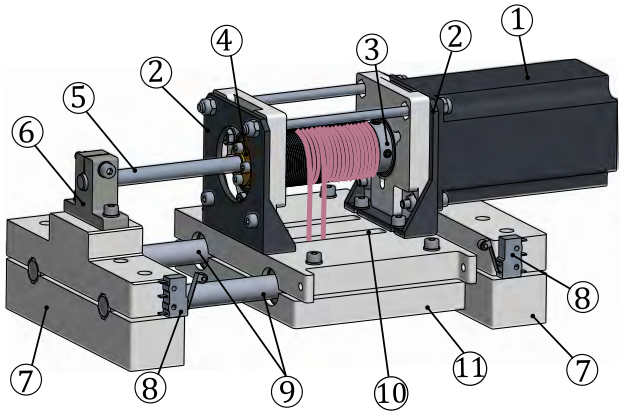

Figure 9. 3D model of the winch: (1) servo-stepper motor, (2) brackets, (3) aluminum drum, (4) brass nut, (5) screw shaft, (6) support element, (7) base plates, (8) end-stop switches, (9) circular rods, (10) cable guidance slot, (11) carriage.

A double-helicoidal-groove aluminum drum (3) is rigidly connected to the shaft of a Wantai (57HBM20-1000, 2.1 Nm holding torque) Nema 23 servo-stepper motor (1) equipped with an incremental encoder ($\approx 0.1^\circ$ resolution). Drum dimensions were chosen in order to coil 2.2 m of a 0.51 mm diameter dyneema cable (DAIWA j-braid X8, 550 N breaking tension), and limit (for the given motor) the realizable maximum tension to 160 N (cable tension safety factor of ≈ 3.5). Thus, drum diameter was selected as 27 mm, and groove pitch as 2 mm. A brass nut (4) is rigidly centered to the drum and coupled to a trapezoidal screw shaft (5), which is clamped at one end to the actuation unit frame, in a support element (6). While the motor rotates, the drum-motor system, fixed to a carriage (11) using two brackets (2), moves on a linear guide (9) made by two circular rods and linear ball

bearings. The drum and the shaft have the same pitch, so the cable portions exiting the drum always have a fixed direction and position with respect to the winch frame. Two end-stop switches (8) are mounted at the physical limits of the drum-motor system, to provide a safety-stop signal to the motor controller. The winch frame is ultimately fixed to the overall robot frame with bolted connections via two plates (7).

This winch houses one of the four cables. One end of the cable is fixed to the drum employing a screw. Then, the cable is coiled onto the first start of the drum and conveyed to the guidance system through a thin slot (10) on the carriage (11). After being guided to the distal anchor point on the platform (as detailed in Section 3.2), the cable returns to the drum through the slot (10) and is then wound onto the other start of the drum and secured with another screw.

3.2. Guidance System

The cable guidance system is designed to (i) guide each of the four cables on a parallelogram-like routing (Figure 10) to ensure the motion of the *EE* in a defined plane; (ii) geometrically define the cable exit points, to apply a standard kinematic model for robot control, (iii) integrate a load sensor for cable tension measurement.

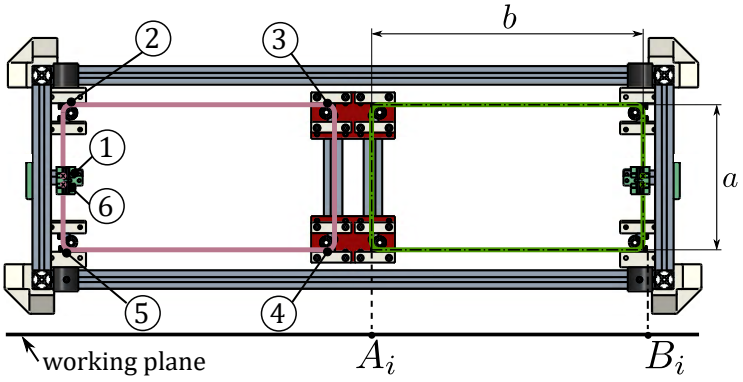

Figure 10. Layout of the guidance system of the robot in standard cable arrangement (top view): (1), (6) fixed pulleys, and (2), (3), (4), (5) swivel pulleys; *a* and *b* sides of the parallelogram defined by the cable loop.

The cable, which leaves the drum groove from a fixed point in space, in a fixed direction (see Section 3.1), is then guided on a fixed pulley (1) attached to a tension measurement unit, which will be analyzed later on. After that, to obtain a parallelogram shape, the cable passes through four identical swivel pulleys (2,3,4,5) and then, through another fixed pulley (6) (also included in the tension measurement unit) before engaging the other groove on the drum. The proposed cable-loop arrangement realized with one cable avoids possible cable slackness during *EE* motion, which may happen if the parallelogram is made of two separate cables driven by the same winch. Two of the swivel pulleys (2,5) are fixed to the base and form the proximal guidance unit, while the other two (3,4) are attached to the platform and form the distal guidance unit. The distance *a* between the two pulleys composing each group is equal. This defines the first two sides of the parallelogram, which are invariant, being distances between points of rigid bodies. The other two sides *b* are formed by cable sections that are equal and parallel when the cable is taut by design.

3.2.1. Sensor Integration

The *CDPR* guidance system is often equipped with position [47] and force sensors [48] to monitor the robot performance in real-time, if required by the control strategy. In this prototype, one of the swivel pulleys of the proximal group is equipped with an incremental encoder. The encoder is coaxial with the swivel pulley, thus it measures the angle between the cable and the frame: this feature can be used for platform pose estimation through direct kinematics [49]. In addition, the fixed pulleys of the proximal guidance group are

equipped with a load sensor, a shear beam load cell (Phidget CZL635 micro load-cell, load range 20 kg). Figure 11 shows the force measurement unit: the load cell (1) is directly connected to the pulley support (2) and structurally constraints the fixed pulleys (3) to the machine frame (4) via an auxiliary bracket (5). The system is designed for the load direction of the pulley to be always orthogonal to the shear beam load cell, to ensure the optimal working conditions of the sensor. The load cell, ideally, measures the double of the cable tension value.

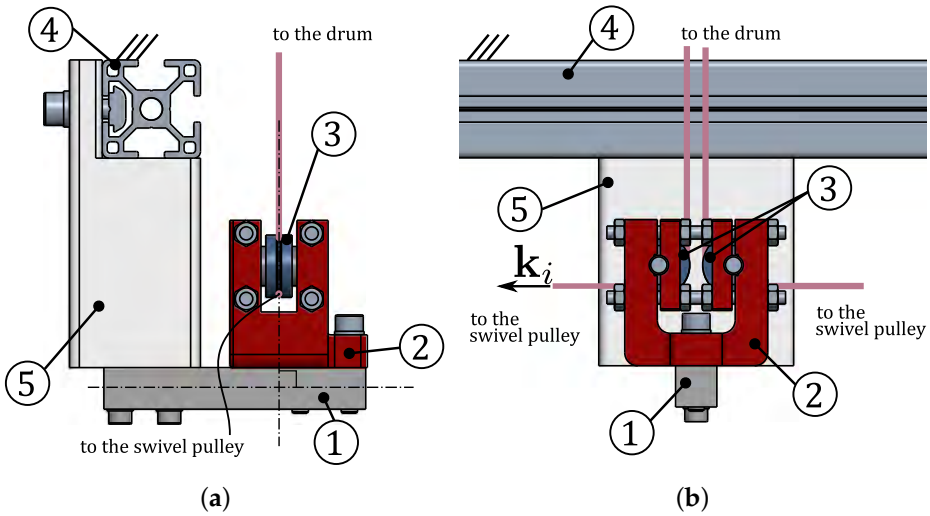

Figure 11. Force measurement unit: (1) load cell, (2) pulley support, (3) fixed pulleys, (4) machine frame, (5) auxiliary bracket. (**a**) Front view. (**b**) Side view.

3.2.2. Kinematic Model

To define the cable exit points, each of the four swivel pulleys forming the guidance system is oriented so that its swivel axis, identified by the unit vector $\mathbf{k}_i$ (Figures 11b and 12b) is orthogonal to the work plane, that is a vertical plane. The two pulleys, forming the proximal or distal guidance units, are coaxial, and the projection of their swivel axes onto the vertical plane identifies the cable exit points (B_i, for $i = 1, \ldots, 4$ for the proximal point in Figure 12a,b). Thus, the kinematic *standard* model can be used without causing geometrical modeling errors. Angle ϕ defines the rotation of the pulley about the swivel axis. $\mathbf{t}_i$ is the unit vector of the i-th cable.

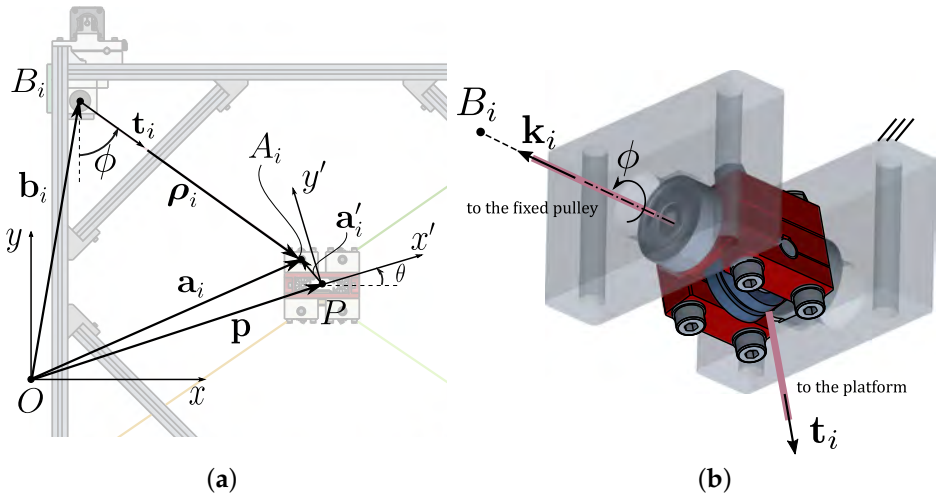

Figure 12. Standard model definition. (**a**) Geometry of the i-th constraint of the planar 4-cable *CDPR*. (**b**) Detail of a proximal swivel pulley.

Considering one of the four cable transmissions (Figure 12), Oxy and $Px'y'$ are defined as inertial and mobile frames. The mobile frame is attached to the platform center of mass P, described as $\mathbf{p}$ with respect to the inertial frame. Cables, assumed massless and inextensible, are considered as the line segments between the distal and proximal anchor points, defined by the pulley swivel axes (A_i and B_i respectively, for $i = 1, \ldots, 4$). Points B_i are described by vectors $\mathbf{b}_i$ in the inertial frame, and points A_i are described by $\mathbf{a'}_i$ and $\mathbf{a'}$ in the mobile and inertial frame, respectively. The rotation matrix $\mathbf{R}(\theta)$ represents the orientation of the moving platform in the vertical plane. The platform pose is defined as $[\mathbf{p}^T, \theta]^T$, and i-th cable vector is:

$$\boldsymbol{\rho}_i = \mathbf{a}_i - \mathbf{b}_i = \mathbf{p} + \mathbf{R}(\theta)\mathbf{a'}_i - \mathbf{b}_i, \quad \mathbf{R}(\theta) \triangleq \begin{bmatrix} cos(\theta) & -sin(\theta) \\ sin(\theta) & cos(\theta) \end{bmatrix} \tag{1}$$

For a given EE pose, the i-th cable length l_i and unit vector $\mathbf{t}_i$ can be computed as:

$$l_i = \|\boldsymbol{\rho}_i\|, \quad \mathbf{t}_i = \frac{\boldsymbol{\rho}_i}{l_i} \tag{2}$$

4. Experimental Demonstration: Laser Engraving

A prototype of a 3-DoF 4-cable *CDPR* with a *crossed layout* was built at IRMA L@B of the University of Bologna (Figure 13a). It employs 4 of the actuation systems described in Section 3.1, connected to the corners of an aluminum frame, and 4 guidance units, whose distal swivel pulleys are bolted to the robot platform. The *CDPR* has rectangular base (0.875 m × 0.700 m) and mobile platform (0.080 m × 0.100 m). The inertial frame Oxy is located in the center of the base and the moving frame $Px'y'$ is located at the center of the EE, coinciding with its center of mass. Its wrench-feasible translational workspace [50] is represented in Figure 13b with a regular discrete grid of 100 × 100 points, considering the platform mass equal to $m = 2.5$ kg, and $\tau_{min} = 10$ N and $\tau_{max} = 80$ N as cable tension limits.

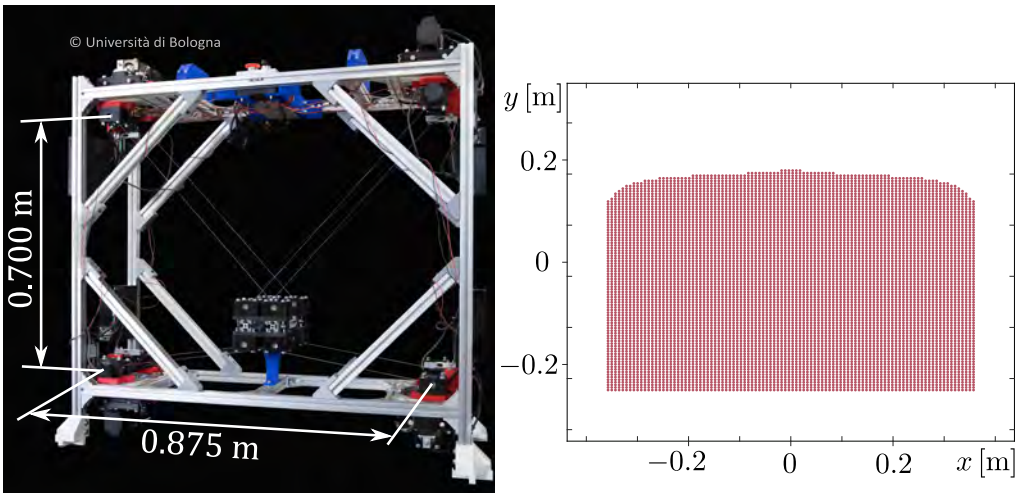

(**a**) (**b**)

Figure 13. Laser-engraving prototype at IRMA L@B. (**a**) Picture of the prototype. (**b**) Wrench-feasible translational workspace of the prototype.

The *CDPR* is controlled by a Real-Time Linux PC, which runs its control algorithm at 1 kHz rate, and feeds motor commands through Ethercat protocol [51] to low-level servo drives. The low-level controller is also developed in-house and run on a ST Nucleo-H743ZI development board at 10 kHz: in addition to controlling motor angles, this allows to directly feed a cable-tension command to the drive. This latter feature simplifies the adoption of the hybrid-input control strategy for the *CDPR* described in [50]: once an

EE-pose set-point is assigned in the Cartesian space, 3 cables are length controlled (i.e., motor angles are commanded to the drives), and one cable is tension controlled (i.e., cable tension is commanded to the drive, and the error with respect to the readings of the load cell is compensated).

A 2.5 W laser diode is mounted on the robot *EE* so that its focal axis is perpendicular to the working plane (Figure 14), thus allowing the engraving of a paper sheet (for additional details, see Supplementary Video Material). The name of our laboratory, IRMA L@B, was stylized in a way that every letter was a union of a finite number of linear segments (Figure 15a): accordingly, a quantitative comparison between the digital model and the engraved result could be performed, by comparing each segment length. A series of consecutive points P_1, $P_2, \ldots$, P_n, with $n = 15$, were extracted from the digital model (Figure 15b), and the robot reference point commanded to follow the path between them with a trapezoidal velocity profile in the task space, while keeping the orientation identically zero. If the trajectory is expressed as:

$$\mathbf{p}(t) = \mathbf{p}_i + (\mathbf{p}_{i+1} - \mathbf{p}_i)u(t), \qquad u(0) = 0,\ u(T) = 1, \qquad i = 1, \ldots, n-1 \tag{3}$$

the motion law $u(t)$ [52] takes the form:

$$u(t) = \begin{cases} \frac{1-\alpha}{2\alpha}(vt)^2, & \text{for } 0 \le t < \alpha T \\ -\frac{\alpha}{2(1-\alpha)} + vt, & \text{for } \alpha T \le t < (1-\alpha)T, \\ -\frac{2\alpha^2-2\alpha+1}{2\alpha(1-\alpha)} + \frac{1}{\alpha}vt - \frac{1-\alpha}{2\alpha}(vt)^2, & \text{for } (1-\alpha)T \le t \le T \end{cases} \qquad T = \frac{1}{v(1-\alpha)} \tag{4}$$

Since the set-points P_i of Equation (3) are set by the task, the only parameters to be determined are v and α of Equation (4). They represent, respectively, the motion law maximum speed, and the ratio between the accelerating phase duration and the total time; they are set considering the requirements of the technological operation to be performed. Since the diode laser can only be on or off, the accelerating phase duration should be as limited as possible, to avoid burning the paper when the *EE* is moving too slow; on the other hand, motors have limited power, and too quick accelerations may result in their stall: by trial and error, $\alpha = 0.1$ was established as a good compromise. The motion law maximum speed was instead calculated so as the *EE* maximum translational speed was optimal for the engraving operation, namely $\|\dot{\mathbf{p}}\|_{max} = 0.02$ m/s for the 2.5 W laser diode at hand; thus, by differentiating Equations (3) and (4) we get:

$$\|\dot{\mathbf{p}}\|_{max} = 0.02 = \|\mathbf{p}_{i+1} - \mathbf{p}_i\|v \tag{5}$$

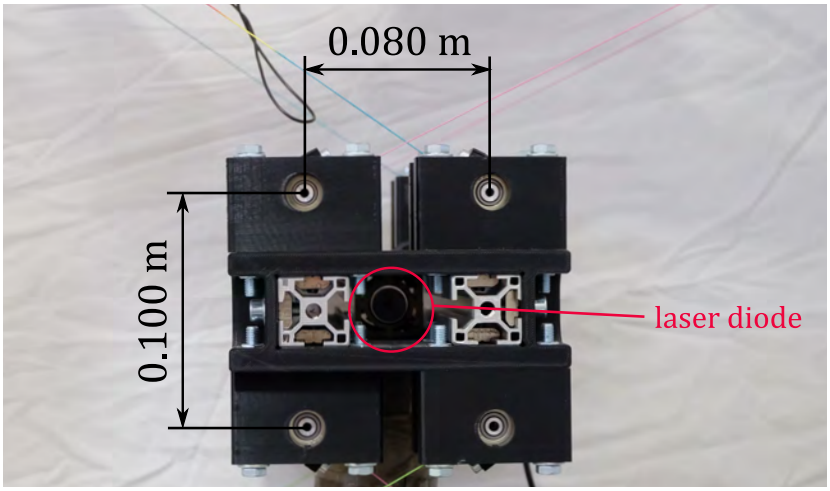

Figure 14. Robot end-effector equipped with a laser diode.

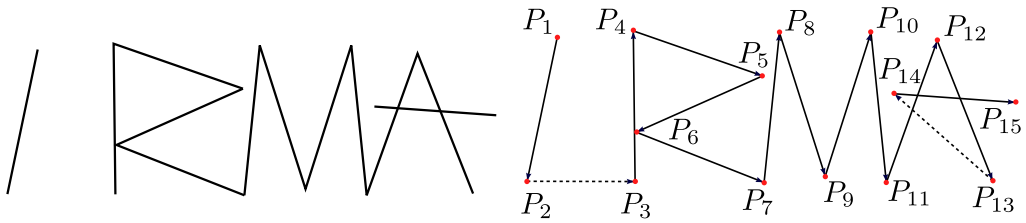

Figure 15. Digital image for engraving task. (**a**) Stylized version of IRMA. (**b**) End-effector path: solid line for engraving process, dotted line for movement; P_i, with $i = 1, \ldots, 15$, consecutive points extracted from the digital image.

The engraving operation of the stylized *IRMA L@B* was then performed, and the result is shown in Figure 16. First of all, it can be noticed that rectilinearity of the segments is qualitatively good (see Figure 17a). Small out-of-plane vibrations were excited by the laser diode cooling fan when the laser was switched on and off at the beginning and the end of each segment. This is nearly unnoticeable even scaling up the engraved paper (see Figure 17b), and it was ultimately expected: a vibration-damping device, such as the one proposed in [27], can be added to prevent such small-magnitude effects.

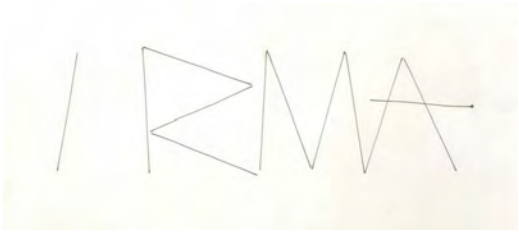

Figure 16. Result of the laser engraving operation.

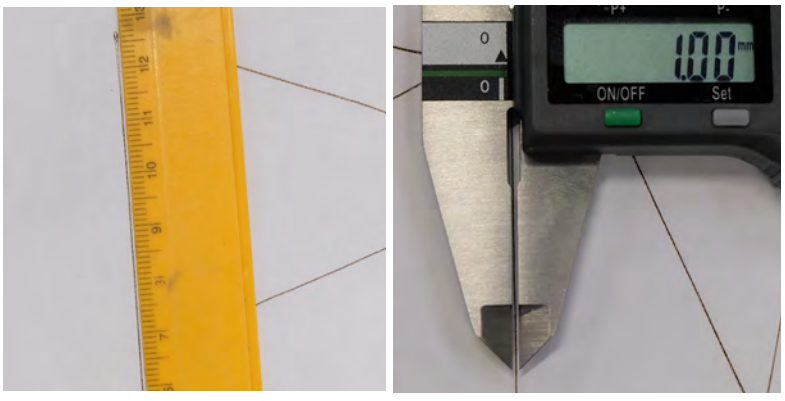

Figure 17. Qualitative evaluation of the laser engraving operation. (**a**) Rectilinearity of a segment. (**b**) Platform out-of-plane oscillations induce sub-millimetric errors.

From a quantitative point of view, the ideal length $l_i^\star$ of each segment was compared to the engraved one l_i, measured on the paper with a digital caliper (maximum measuring error of 0.3 mm at full scale, 180 mm). If the error is defined as $\epsilon_{l_i} = l_i^\star - l_i$ and the percentage error is $\epsilon_{l_i,\%} = 100(l_i^\star - l_i)/l_i^\star$, the root-mean-square error was 2 mm, and the root-mean-square percentage error was 2.4% (complete results can be found in Table 1). Considering the size of the robot workspace and its prototypal nature (most of the components are 3D printed in plastic material), errors of this magnitude are reasonably attributed to an imperfect calibration, mounting errors of the guidance system on the aluminum

frame, and elastic components deflection. All in all, the machine can perform the planar non-contact task with relatively good accuracy, which can be increased with a more advanced mechanical design, followed by a precise calibration.

Table 1. Comparison between ideal and engraved segment lengths.

i	1	2	3	4	5	6	7	8	9	10	11	12	13	14
$l_i^\star$ [mm]	90.8	66.4	92.7	84.2	85.1	84.6	92.7	92.7	92.7	92.7	92.7	92.7	80.9	75.2
l_i [mm]	89.4	64.4	91.2	87.4	85.5	88.3	91.2	94.6	91.3	91.6	90.5	92.6	78.3	76.9
ϵ_{l_i} [mm]	−1.4	−2.0	−1.5	3.2	0.4	3.7	−1.5	1.9	−1.4	−1.1	−2.2	−0.1	−2.6	1.7
$\epsilon_{l_i,\%}$ [%]	−1.6	−3.1	−1.6	3.7	0.4	4.4	−1.6	2.1	−1.5	−1.2	−2.3	−0.1	−3.3	2.3

5. Conclusions

This paper presented an overconstrained *CDPR* for non-contact tasks on planar vertical surfaces. The actuation and guidance systems were described and the applicability of the standard model was outlined by showing the employed design expedients. The *CDPR* prototype was built at IRMA laboratory at the University of Bologna, and used to perform laser engraving on a paper sheet. Engraving results are qualitatively good, considering the prototypal nature of the robot, and quantitatively acceptable, since they can be improved by better manufacture of mechanical components and calibration.

In the future, the proposed actuation and guidance units design will be evolved in order to achieve on-site deployability: the actuation (or guidance) unit will be mounted on a vertical façade, and the system geometry will be self-calibrated on-site after each mounting operation.

6. Patents

The preliminary design of the prototype presented in this paper is object of the patent WO2021144685.

Supplementary Materials: The following are available at https://www.mdpi.com/2076-3417/11/20/9491/s1, Video S1: This video shows the engraving process described in the experimental section of the paper.

Author Contributions: Conceptualization, V.M. and E.I.; methodology, V.M. and E.I.; software, V.M. and E.I.; validation, V.M. and E.I.; writing—original draft preparation, V.M.; writing—review and editing, V.M. and E.I.; supervision, M.C.; project administration, E.I. and M.C. All authors have read and agreed to the published version of the manuscript.

Funding: This research received no external funding.

Institutional Review Board Statement: Not applicable.

Informed Consent Statement: Not applicable.

Data Availability Statement: Data is contained within the article.

Acknowledgments: The authors would like to acknowledge Federico Zaccaria for his help in designing the prototype components.

Conflicts of Interest: The authors declare no conflict of interest.

References

1. Pott, A. *Cable-Driven Parallel Robots: Theory and Application*; Springer: Berlin/Heidelberg, Germany, 2018; Volume 120.
2. Gagliardini, L.; Caro, S.; Gouttefarde, M.; Wenger, P.; Girin, A. A Reconfigurable Cable-Driven Parallel Robot for Sandblasting and Painting of Large Structures. In *Cable-Driven Parallel Robots*; Pott, A., Bruckmann, T., Eds.; Springer International Publishing: Cham, Switzerland, 2015; pp. 275–291.

3. Piao, J.; Jin, X.; Choi, E.; Park, J.O.; Kim, C.S.; Jung, J. A Polymer Cable Creep Modeling for a Cable-Driven Parallel Robot in a Heavy Payload Application. In *Cable-Driven Parallel Robots*; Gosselin, C., Cardou, P., Bruckmann, T., Pott, A., Eds.; Springer International Publishing: Cham, Switzerland, 2018; pp. 62–72.
4. Idà, E.; Bruckmann, T.; Carricato, M. Rest-to-Rest Trajectory Planning for Underactuated Cable-Driven Parallel Robots. *IEEE Trans. Robot.* **2019**, *35*, 1338–1351. [CrossRef]
5. Idà, E.; Briot, S.; Carricato, M. Robust Trajectory Planning of Under-Actuated Cable-Driven Parallel Robot with 3 Cables. In *Advances in Robot Kinematics 2020*; Lenarčič, J., Siciliano, B., Eds.; Springer International Publishing: Cham, Switzerland, 2021; pp. 65–72.
6. Brown, G.W. Suspension System for Supporting and Conveying Equipment, such as a Camera. U.S. Patent 4,710,819, 1 December 1987.
7. Abdolshah, S.; Zanotto, D.; Rosati, G.; Agrawal, S. Performance evaluation of a new design of cable-suspended camera system. In Proceedings of the 2017 IEEE International Conference on Robotics and Automation (ICRA), Singapore, 29 May–3 June 2017; pp. 3728–3733.
8. Bruckmann, T.; Lalo, W.; Nguyen, K.; Salah, B. Development of a Storage Retrieval Machine for High Racks Using a Wire Robot. In Proceedings of the International Design Engineering Technical Conferences and Computers and Information in Engineering Conference, Chicago, IL, USA, 12–15 August 2012; Volume 4, pp. 771–780.
9. Pott, A.; Meyer, C.; Verl, A. Large-scale assembly of solar power plants with parallel cable robots. In Proceedings of the ISR 2010 (41st International Symposium on Robotics) and ROBOTIK 2010 (6th German Conference on Robotics), Munich, Germany, 7–9 June 2010; pp. 1–6.
10. Izard, J.B.; Dubor, A.; Hervé, P.E.; Cabay, E.; Culla, D.; Rodriguez, M.; Barrado, M. Large-scale 3D printing with cable-driven parallel robots. *Construct. Robot.* **2017**, *1*, 69–76. [CrossRef]
11. Bruckmann, T.; Boumann, R. Simulation and optimization of automated masonry construction using cable robots. *Adv. Eng. Inf.* **2021**, *50*, 101388. [CrossRef]
12. Izard, J.B.; Gouttefarde, M.; Baradat, C.; Culla, D.; Sallé, D. Integration of a Parallel Cable-Driven Robot on an Existing Building Façade. In *Cable-Driven Parallel Robots*; Bruckmann, T., Pott, A., Eds.; Springer: Berlin/Heidelberg, Germany, 2013; pp. 149–164.
13. De Zeeuw, D.; Spanjer, S.A.J.; Zeggelaar, K. Cleaning System for a Façade of a Building Structure. International Patent WO 2016/085330, 2 June 2016.
14. Pott, A.; Mütherich, H.; Kraus, W.; Schmidt, V.; Miermeister, P.; Verl, A. IPAnema: A family of Cable-Driven Parallel Robots for Industrial Applications. In *Cable-Driven Parallel Robots*; Bruckmann, T., Pott, A., Eds.; Springer: Berlin/Heidelberg, Germany, 2013; pp. 119–134.
15. Gouttefarde, M.; Collard, J.F.; Riehl, N.; Baradat, C. Geometry Selection of a Redundantly Actuated Cable-Suspended Parallel Robot. *IEEE Trans. Robot.* **2015**, *31*, 501–510. [CrossRef]
16. Idà, E.; Marian, D.; Carricato, M. A Deployable Cable-Driven Parallel Robot with Large Rotational Capabilities for Laser-Scanning Applications. *IEEE Robot. Automat. Lett.* **2020**, *5*, 4140–4147. [CrossRef]
17. Yang, H.; Izard, J.B.; Baradat, C.; Krut, S.; Pierrot, F.; Gouttefarde-tanich, M.; Company, O. Planar Motion Device. U.S. Patent 10,449,668, 22 October 2019.
18. Corral, E.; Moreno, R.G.; García, M.J.G.; Castejón, C. Nonlinear phenomena of contact in multibody systems dynamics: A review. *Nonlinear Dyn.* **2021**, *104*, 1269–1295. [CrossRef]
19. Reichert, C.; Bruckmann, T. Unified Contact Force Control Approach for Cable-driven Parallel Robots using an Impedance/Admittance Control Strategy. In Proceedings of the 14th IFToMM World Congress, Taipei, Taiwan, 25–30 October 2015; pp. 645–654.
20. Vu, D.S.; Barnett, E.; Zaccarin, A.M.; Gosselin, C. On the Design of a Three-DOF Cable-Suspended Parallel Robot Based on a Parallelogram Arrangement of the Cables. In *Cable-Driven Parallel Robots*; Gosselin, C., Cardou, P., Bruckmann, T., Pott, A., Eds.; Springer International Publishing: Cham, Switzerland, 2018; pp. 319–330.
21. Mottola, G.; Gosselin, C.; Carricato, M. Effect of Actuation Errors on a Purely-Translational Spatial Cable-Driven Parallel Robot. In Proceedings of the 2019 IEEE 9th Annual International Conference on CYBER Technology in Automation, Control, and Intelligent Systems (CYBER), Suzhou, China, 29 July–2 August 2019; pp. 701–707.
22. Khodadadi, N.; Hosseini, M.I.; Khalilpour, S.A.; Taghirad, H.D.; Cardou, P. Multi Objective Optimization of a Cable-Driven Robot with Parallelogram Links. In *Cable-Driven Parallel Robots*; Gouttefarde, M., Bruckmann, T., Pott, A., Eds.; Springer International Publishing: Cham, Switzerland, 2021; pp. 170–181.
23. Torres-Mendez, S.; Khajepour, A. Analysis of a High Stiffness Warehousing Cable-Based Robot. In Proceedings of the International Design Engineering Technical Conferences and Computers and Information in Engineering Conference, Buffalo, NY, USA, 17–20 August 2014; Volume 5A.
24. Bosscher, P.; Williams, R.L.; Tummino, M. A Concept for Rapidly-Deployable Cable Robot Search and Rescue Systems. In Proceedings of the ASME 2005 International Design Engineering Technical Conferences and Computers and Information in Engineering Conference, Long Beach, CA, USA, 24–28 September 2005; pp. 589–598.
25. Bosscher, P.; Williams, R.L.; Bryson, L.S.; Castro-Lacouture, D. Cable-Suspended Robotic Contour Crafting System. In Proceedings of the International Design Engineering Technical Conferences and Computers and Information in Engineering Conference, Philadelphia, PA, USA, 10–13 September 2006; pp. 777–785.

26. Wahle, S. Storage System, in Particular Rack Storage. Deutsches DE Patent 10 2010 015 530, 6 September 2021.
27. De Rijk, R.; Rushton, M.; Khajepour, A. Out-of-Plane Vibration Control of a Planar Cable-Driven Parallel Robot. *IEEE/ASME Trans. Mechatron.* **2018**, *23*, 1684–1692. [CrossRef]
28. Idà, E.; Briot, S.; Carricato, M. Natural Oscillations of Underactuated Cable-Driven Parallel Robots. *IEEE Access* **2021**, *9*, 71660–71672. [CrossRef]
29. Wang, D.; Ahn, J.; Jung, J.; Seon, J.A.; Park, J.O.; Ko, S.Y.; Park, S. Winch-integrated mobile end-effector for a cable-driven parallel robot with auto-installation. *Int. J. Control Automat. Syst.* **2017**, *15*, 2355–2363. [CrossRef]
30. Bruckmann, T.; Mikelsons, L.; Brandt, T.; Hiller, M.; Schramm, D. Wire Robots Part I: Kinematics, Analysis & Design. In *Parallel Manipulators*; Ryu, J.H., Ed.; IntechOpen: Rijeka, Croatia, 2008; Chapter 6.
31. Reichert, C.; Bruckmann, T. Optimization of the Geometry of a Cable-Driven Storage and Retrieval System. In *Robotics and Mechatronics*; Yang, R., Takeda, Y., Zhang, C., Fang, G., Eds.; Springer International Publishing: Cham, Switzerland, 2019; pp. 225–237.
32. Pott, A. Influence of Pulley Kinematics on Cable-Driven Parallel Robots. In *Latest Advances in Robot Kinematics*; Lenarcic, J., Husty, M., Eds.; Springer: Dordrecht, The Netherlands, 2012; pp. 197–204.
33. Merlet, J.P. Comparison of Actuation Schemes for Wire-Driven Parallel Robots. In *New Trends in Mechanism and Machine Science*; Viadero, F., Ceccarelli, M., Eds.; Springer: Dordrecht, The Netherlands, 2013; pp. 245–254.
34. Merlet, J.P. MARIONET, A Family of Modular Wire-Driven Parallel Robots. In *Advances in Robot Kinematics: Motion in Man and Machine*; Lenarcic, J., Stanisic, M.M., Eds.; Springer: Dordrecht, The Netherlands, 2010; pp. 53–61.
35. Surdilovic, D.; Bernhardt, R. STRING-MAN: A new wire robot for gait rehabilitation. In Proceedings of the IEEE International Conference on Robotics and Automation, ICRA'04, New Orleans, LA, USA, 26 April–1 May 2004; Volume 2, pp. 2031–2036.
36. Feyrer, K. *Wire Ropes: Tension, Endurance, Reliability*; Springer Science & Business Media: Berlin/Heidelberg, Germany 2015.
37. Pham, C.B.; Yang, G.; Yeo, S.H. Dynamic analysis of cable-driven parallel mechanisms. In Proceedings of the 2005 IEEE/ASME International Conference on Advanced Intelligent Mechatronics, Monterey, CA, USA, 24–28 July 2005; pp. 612–617.
38. Izard, J.B.; Gouttefarde, M.; Michelin, M.; Tempier, O.; Baradat, C. A Reconfigurable Robot for Cable-Driven Parallel Robotic Research and Industrial Scenario Proofing. In *Cable-Driven Parallel Robots*; Bruckmann, T., Pott, A., Eds.; Springer: Berlin/Heidelberg, Germany, 2013; pp. 135–148.
39. Rognant, M.; Courteille, E. Improvement of Cable Tension Observability Through a New Cable Driving Unit Design. In *Cable-Driven Parallel Robots*; Gosselin, C., Cardou, P., Bruckmann, T., Pott, A., Eds.; Springer International Publishing: Cham, Switzerland, 2018; pp. 280–291.
40. von Zitzewitz, J.; Fehlberg, L.; Bruckmann, T.; Vallery, H. Use of Passively Guided Deflection Units and Energy-Storing Elements to Increase the Application Range of Wire Robots. In *Cable-Driven Parallel Robots*; Bruckmann, T., Pott, A., Eds.; Springer: Berlin/Heidelberg, Germany, 2013; pp. 167–184.
41. Fang, S.; Franitza, D.; Torlo, M.; Bekes, F.; Hiller, M. Motion control of a tendon-based parallel manipulator using optimal tension distribution. *IEEE/ASME Trans. Mechatron.* **2004**, *9*, 561–568. [CrossRef]
42. Ottaviano, E.; Ceccarelli, M.; De Ciantis, M. A 4–4 cable-based parallel manipulator for an application in hospital environment. In Proceedings of the 2007 Mediterranean Conference on Control Automation, Athens, Greece, 27–29 June 2007; pp. 1–6.
43. Kraus, W.; Kessler, M.; Pott, A. Pulley friction compensation for winch-integrated cable force measurement and verification on a cable-driven parallel robot. In Proceedings of the 2015 IEEE International Conference on Robotics and Automation (ICRA), Seattle, WA, USA, 26–30 May 2015; pp. 1627–1632.
44. Hiller, M.; Fang, S.; Mielczarek, S.; Verhoeven, R.; Franitza, D. Design, analysis and realization of tendon-based parallel manipulators. *Mech. Mach. Theory* **2005**, *40*, 429–445. [CrossRef]
45. Gonzalez-Rodriguez, A.; Castillo-Garcia, F.J.; Ottaviano, E.; Rea, P.; Gonzalez-Rodriguez, A.G. On the effects of the design of cable-Driven robots on kinematics and dynamics models accuracy. *Mechatronics* **2017**, *43*, 18–27. [CrossRef]
46. Gouttefarde, M.; Krut, S.; Company, O.; Pierrot, F.; Ramdani, N. On the Design of Fully Constrained Parallel Cable-Driven Robots. In *Advances in Robot Kinematics: Analysis and Design*; Lenarčič, J., Wenger, P., Eds.; Springer: Dordrecht, The Netherlands, 2008; pp. 71–78.
47. Idá, E.; Merlet, J.P.; Carricato, M. Automatic Self-Calibration of Suspended Under-Actuated Cable-Driven Parallel Robot using Incremental Measurements. In *Cable-Driven Parallel Robots*; Pott, A., Bruckmann, T., Eds.; Springer International Publishing: Cham, Switzerland, 2019; pp. 333–344.
48. Yang Ho, W.; Kraus, W.; Mangold, A.; Pott, A. Haptic Interaction with a Cable-Driven Parallel Robot Using Admittance Control. In *Cable-Driven Parallel Robots*; Pott, A., Bruckmann, T., Eds.; Springer International Publishing: Cham, Switzerland, 2015; pp. 201–212.
49. Merlet, J.P. Direct Kinematics of CDPR with Extra Cable Orientation Sensors: The 2 and 3 Cables Case with Perfect Measurement and Ideal or Elastic Cables. In *Cable-Driven Parallel Robots*; Gosselin, C., Cardou, P., Bruckmann, T., Pott, A., Eds.; Springer International Publishing: Cham, Switzerland, 2018; pp. 180–191.
50. Mattioni, V.; Idà, E.; Carricato, M. Force-Distribution Sensitivity to Cable-Tension Errors: A Preliminary Investigation. In *Cable-Driven Parallel Robots*; Gouttefarde, M., Bruckmann, T., Pott, A., Eds.; Springer International Publishing: Cham, Switzerland, 2021; pp. 129–141.

51. Boschetti, G.; Minto, R.; Trevisani, A. Experimental Investigation of a Cable Robot Recovery Strategy. *Robotics* **2021**, *10*, 35. [CrossRef]
52. Biagiotti, L.; Melchiorri, C. *Trajectory Planning for Automatic Machines and Robots*; Springer Science & Business Media: Berlin/Heidelberg, Germany, 2008.